Available online at www.sciencedirect.com
SCIENCE DIRECT®
Journal of volcanology and geothermal research
ELSEVIER
Journal of Volcanology and Geothermal Research 123 (2003) 301–312
www.elsevier.com/locate/jvolgeores

# Morphological analysis of active Mount Nemrut stratovolcano, eastern Turkey: evidences and possible impact areas of future eruption

Erkan Aydar [a,*], Alain Gourgaud [b,**], Inan Ulusoy [a], Fabrice Digonnet [b], Philippe Labazuy [b], Erdal Sen [a], Hasan Bayhan [a], Turker Kurttas [a], Arif Umit Tolluoglu [c]

[a] *Department of Geological Engineering, Hacettepe University, 06532, Beytepe-Ankara, Turkey*
[b] *Université Blaise Pascal, UMR–CNRS 6524, 5 rue Kessler, 63038 Clermont-Ferrand, France*
[c] *Department of Geological Engineering, Yuzuncuyil University, Van, Turkey*

Received 1 February 2002; accepted 13 December 2002

**Abstract**

Mount Nemrut, an active stratovolcano in eastern Turkey, is a great danger for its vicinity. The volcano possesses a summit caldera which cuts the volcano into two stages, i.e. pre- and post-caldera. Wisps of smoke and hot springs are to be found within the caldera. Although the last recorded volcanic activity is known to have been in 1441, we consider here that the last eruption of Nemrut occurred more recently, probably just before 1597. The present active tectonic regime, historical eruptions, occurrence of mantle-derived magmatic gases and the fumarole and hot spring activities on the caldera floor make Nemrut Volcano a real danger for its vicinity. According to the volcanological past of Nemrut, the styles of expected eruptions are well-focused on two types: (1) occurrence of water within the caldera leads to phreatomagmatic (highly energetic) eruptions, subsequently followed by lava extrusions, and (2) effusions–extrusions (non-explosive or weakly energetic eruptions) on the flanks from fissures. To predict the impact area of future eruptions, a series of morphological analyses based on field observations, Digital Elevation Model and satellite images were realized. Twenty-two valleys (main transport pathways) were classified according to their importance, and the physical parameters related to the valleys were determined. The slope values in each point of the flanks and the Heim parameters $H/L$ were calculated. In the light of morphological analysis the possible impact areas around the volcano and danger zones were proposed. The possible transport pathways of the products of expected volcanic events are unified in three main directions: Bitlis, Guroymak, Tatvan and Ahlat cities, the about 135 000 inhabitants of which could be threatened by future eruptions of this poorly known and unsurveyed volcano.


*Keywords:* Turkey; Nemrut; volcano; morphology; image analysis; impact area

## 1. Introduction

Eastern Turkey hosts several poorly known sub-active/active volcanoes like Mount Ararat,

* Corresponding author.
** Corresponding author.
*E-mail addresses:* eaydar@hacettepe.edu.tr (E. Aydar), gourgaud@opgc.univ-bpclermont.fr (A. Gourgaud).

0377-0273/03/$ – see front matter © 2003 Elsevier Science B.V. All rights reserved.
doi:10.1016/S0377-0273(03)00002-7

Mount Tendurek, Mount Suphan and Mount Nemrut (Yilmaz et al., 1998). All witnessed volcanic activity during the Late Pleistocene and/or Holocene. The area still experiences tectonic deformations related to the collision of the Arabian and Eurasian plates (Dewey et al., 1986). In this active tectonic context, Nemrut Volcano is located at the eastern end of the Mus Basin (Yilmaz et al., 1987) (Fig. 1a). However, radiometric ages collected from the literature show that the volcano has been active for the last 1.2 Ma; most of the volcanics are younger than 500 ka. Although the last volcanic activity is known to have occurred in 1441 (Oswalt, 1912; Pfaffengolz, 1950), we found a live description of the last eruption of Nemrut in an Arabic book written in 1597 (Serefhan, 1597). The Turkish translator of the mentioned book provides a note stating that the original version of this book called 'Serefname' is in the Bodleian Library of Oxford University, UK (registration number 312). We decided to quote the text as it is in the Turkish translation of the mentioned book. Remarks in parentheses are our own comments.

'(Mythological description) *To the north of Bedlis* (actual Bitlis City)*, between the cities of Mus and Ahlat, there is a high mountain called 'Nemruz'* (actual Nemrut). *Natives believe that Nemruz* (the king) *used to spend the winters around and the summers on this mountain. For this purpose, he had a castle and a palace built on the summit. He used to live and spend lots of time there. He fell victim to God's wrath and got caught. Consequently, the god let this mountain, the height of which was not less than 2000 zira* (ancient length unit: 1 zira = 0.757738 m)*, collapse and sink 1500 zira* (caldera collapse).

(Live description of Nemrut) *This sinking created a lake of 5000 zira wide. Its water is crystal clear and extremely cool. It is strange that when digging a pit on its banks hot water spouts upward.*

*The land is stony. There is neither much soil nor much mud. Because the black rocks* (obsidian flows) *lay next to each other. Some of these rocks are of a kind called camel's eye by Turks. They are hard and do resemble filled honeycombs* (spherulitic obsidian; Fig. 1e)*. In addition, there is another kind of stone which is softer than the others, like dark rocks* (dark-colored ignimbrites).

(Live description of the eruption) *In the northern part of this location there is a canal* (fissure) *through which flows a dark water* (basaltic magma). *It resembles the dark water which flows off the blacksmith's bellows and its weight is heavier than iron. It spouts upward and quickly flows down to the gorge. According to me, each year this water increases and decreases. It jets more than 30 zira* (lava fountain), *and spreads around longer than 100 zira* (ejecta). *And here it spouts out from several points* (rift zone)*. Whoever has the intention to separate part of this water will face great difficulties* (hard basaltic rock)'.

As Nemrut represents historical volcanism as well as current fumarole activity, we aim to investigate the volcanological and morphological features of Mount Nemrut in this paper. A scenario of possible volcanic events expected to occur in future and their impact areas will be discussed.

## 2. Volcanological past of Mount Nemrut

Mount Nemrut stratovolcano, which culminates at 2948 m, is situated on the western shore of Lake Van (1648 m above sea level), a soda lake covering a surface of 3574 km$^2$ (Fig. 1). The volcano exhibits a summit caldera, the surface area of which is 8.5×7 km. The eastern half of the caldera is filled by pyroclastic deposits related to maar-like explosion craters (Fig. 1b), lava domes and flows. The western half is filled by a freshwater lake covering a surface area of 5.3×3 km and a small lake with hot springs (Fig. 1). The average depth of the larger lake is estimated to be 100 m, although the maximum depth is close to 156 m (Ozpeker, 1973). The fumarole activity is

Fig. 1. Georeferenced SPOT image. (a) DEM of Turkey and the location of Mount Nemrut Volcano. (b) Field view of intracaldera phreatomagmatic products. (c) Fumarole activity at the caldera floor. (d) A view of the caldera interior with obsidian flow and lake. (e) Spherulite occurrences on the obsidian flow. (f) A general view of Bitlis valley.

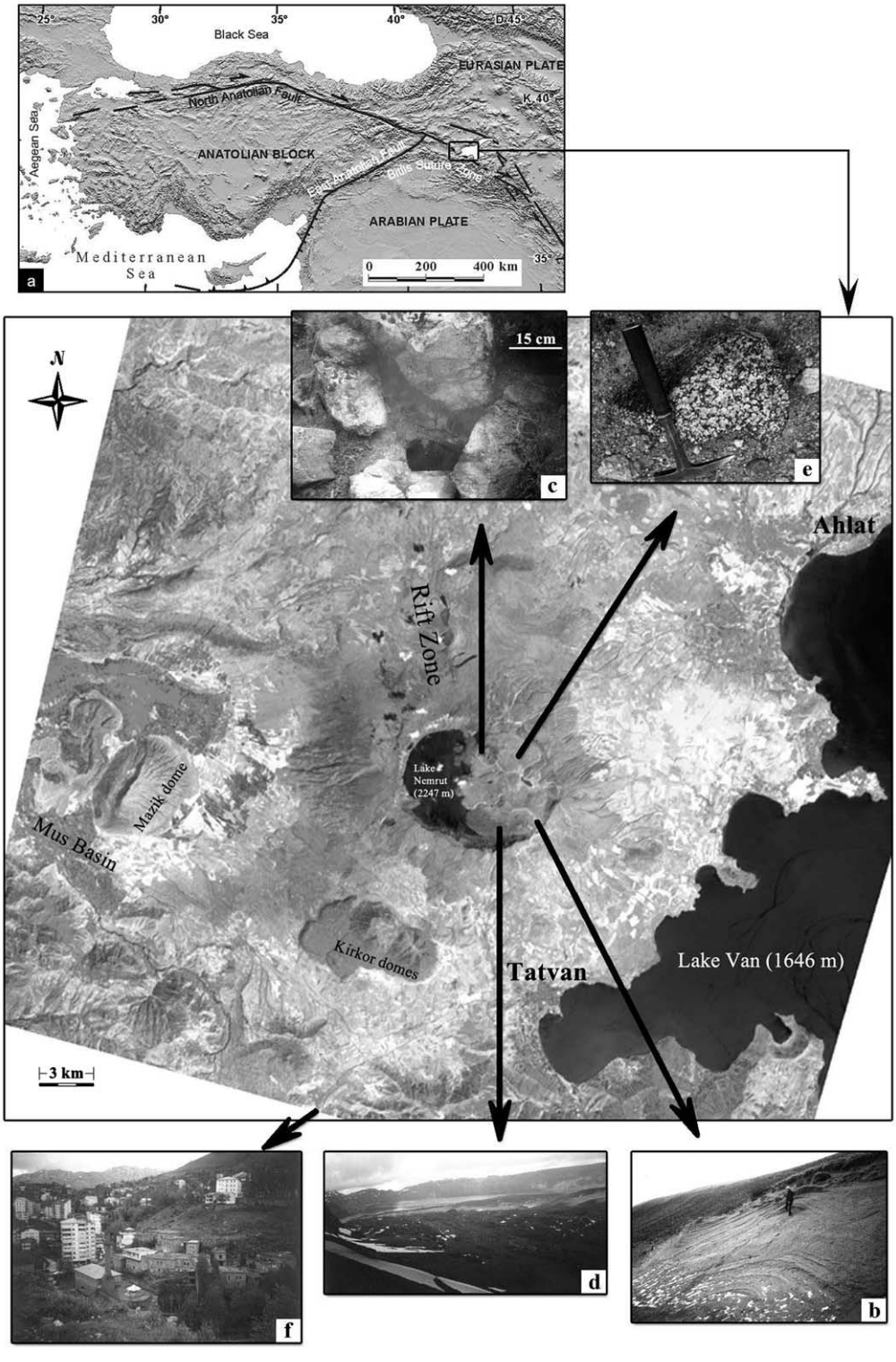
25°
30°
35°
40°
45°
Black Sea
EURASIAN PLATE
North Anatolian Fault
40°
Aegean Sea
ANATOLIAN BLOCK
East Anatolian Fault
Bitlis Suture Zone
ARABIAN PLATE
Mediterranean Sea
0 200 400 km
35°
a
15 cm
c
e
N
Ahlat
Rift Zone
Lake Nemrut (2247 m)
Mazik dome
Mus Basin
Kirkor domes
Tatvan
Lake Van (1646 m)
3 km
f
d
b

also present over a dome situated at the northern part of the caldera (Fig. 1c). A $^{3}He/^{4}He$ isotopic ratio measurement on the hot spring indicates that the gases are actually released directly from the mantle-derived magma (Nagao et al., 1989). Mount Nemrut, however, is poorly known in the literature, but was previously investigated in Yilmaz et al. (1998), who proposed five evolutionary phases for all East Anatolian volcanoes (the stratovolcanoes of Mount Ararat, Mount Suphan, Mount Nemrut and the shield volcano of Mount Tendurek) as pre-cone, cone building, climactic, post-caldera and late phase. Our stratigraphy and evolutionary stage distinctions are different and we defined two main evolutionary stages in the history of this active volcano, cut by the paroxysmal eruption leading to the caldera collapse (Fig. 2): the pre-caldera and post-caldera stages.

### 2.1. Pre-caldera stage

It can be subdivided into two phases: construction and destruction phases.

#### 2.1.1. Construction phase

This is characterized predominantly by basaltic, trachytic, rhyolitic lava flows, lava dome emplacements and associated block-and-ash flows (Fig. 1). The oldest lavas are fissure-fed basalts related to scoria cones, dated to $1.18 \pm 0.23$ Ma (Pearce et al., 1990). At the southwest and west of the caldera, the dome complex of Kirkor (dated to 0.31 Ma by Ercan et al., 1990) and Mazik were emplaced within the Mus Basin. Measured flanks and slope values lead us to suppose that the summit of this primitive volcano reached about 4500 m high.

#### 2.1.2. Destruction phase

During the destruction phase, the eruption style of the volcano became paroxysmal with important pumiceous plinian-style air-falls which were subsequently followed by welded ignimbrite emplacement. Near Tatvan city, 10 km from the source, the thickness of plinian fall deposits is some tens of meters. The ignimbrites are dark brown colored and exhibit a fiamme texture. They are thin on the slopes of the volcano, only several meters thick, while the thickness increases drastically within the valleys, reaching several tens of meters in the Bitlis valley. The volume of the ignimbrite and its related products is estimated as 40 $km^3$, over an area of 860 $km^2$. Following this paroxysmal event, the caldera collapsed. The surface area of collapse, representing an ellipsoidal shape, corresponds to 45 $km^2$. The volumes of caldera and total collapse are estimated to be 40 $km^3$ and 65 $km^3$, respectively. Although the age of this major event is unknown, we observed the ignimbrites over the Kirkor domes dated to 0.31 Ma by Ercan et al. (1990).

### 2.2. Post-caldera stage

This stage witnessed intracaldera and flank eruptions. The eastern half of the caldera is occupied by phreatomagmatic craters, lava dome and flows (Fig. 1d). At least three explosion craters are recognized. Their tuff-rings exhibit base surge deposits with dune and anti-dune structures, bomb-sags and pool structures, bread-crust bombs and cross-bedding. Trachytic and rhyolitic lavas were extruded within the explosion craters in the forms of either lava flows, dominantly obsidian flows sometimes spherulitic (Fig. 1e), or lava-domes. The radiometric ages of intracaldera volcanism are very young, ranging from $0.02 \pm 0.01$ Ma to $< 10$ ka (Nagao et al., 1989). Fumarole activity and hot springs are still present on the caldera floor.

Basalts and trachytes are dominant among the flank eruption products. Beside the scattered basaltic and trachytic lavas on the flanks, the most spectacular eruptive event is that of the northern flank, where there is a 'rift zone', supposed to have occurred in 1441 (Fig. 1). It is composed of fissural basaltic and trachytic lavas.

## 3. Morphological analysis of Mount Nemrut

Because of present active tectonics, young ages, historical eruptions, occurrence of mantle-derived magmatic gases and fumarole and hot spring activities on the caldera floor, Nemrut Volcano is considered dangerous for its vicinity. According

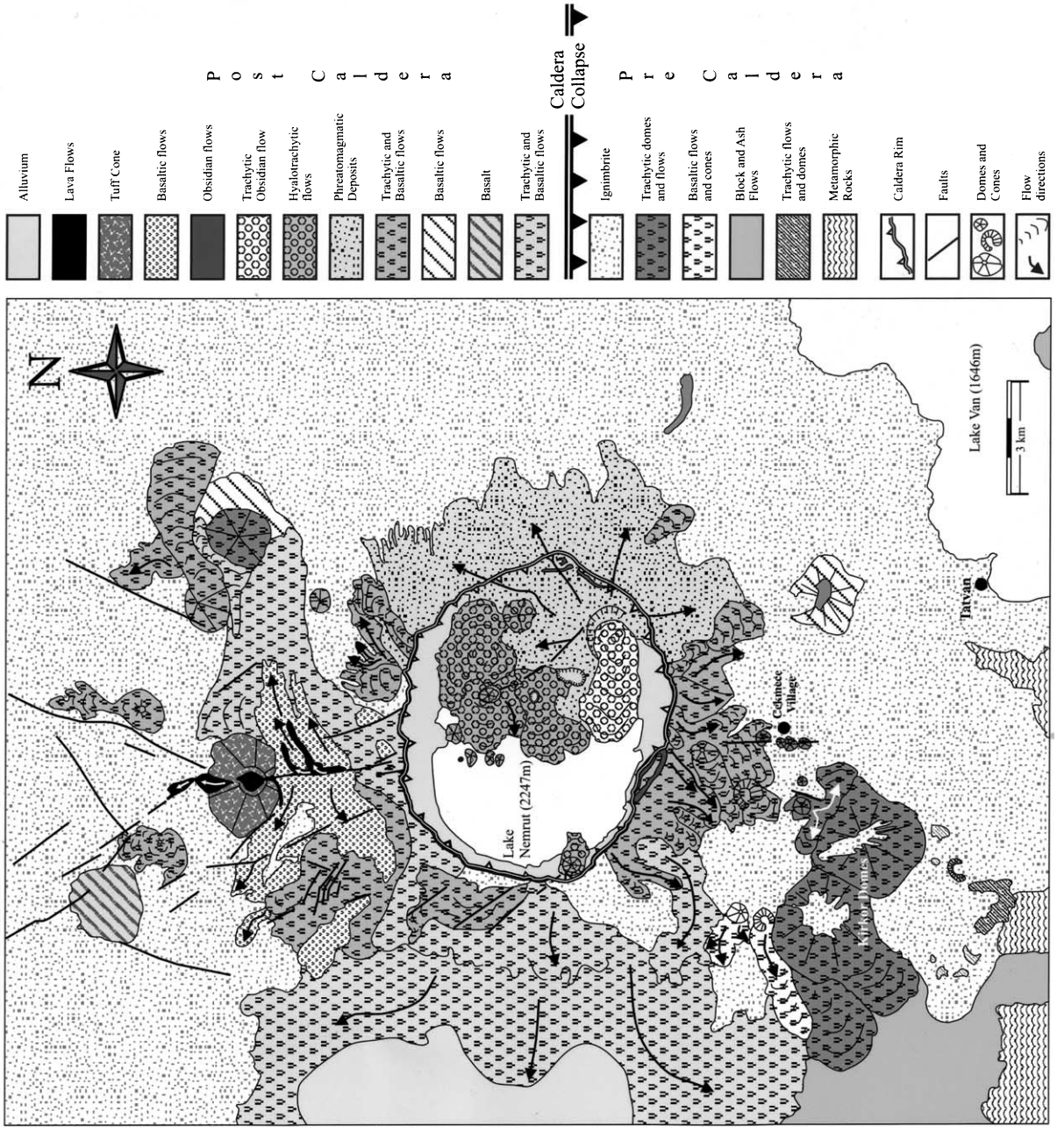


Fig. 2. Geological sketch map of Mount Nemrut (modified from Yilmaz et al., 1998).

to the volcanological past of Nemrut, the styles of expected eruptions are of two types: (1) occurrence of water within the caldera leads to phreatomagmatic (high energy) eruptions, subsequently followed by lava extrusions, and (2) lava effusions or extrusions (non-explosive or low energy eruptions) from the fissures on the flanks. The expected future eruptions could have a great impact on Tatvan city (Fig. 1) (10 km from the summit of the volcano), where the population is 66 000 inhabitants according to the results of Turkey's 1997 census. The other impact areas are Bitlis

Fig. 3. Risk analysis based on DEM of Mount Nemrut. (a) Slope visualization of Mount Nemrut. Dark areas correspond to high slope values. (b) Drainage pattern of volcano. (c) Classification of the steep valleys obtained by overlapping of slope image and valley visualization.

city (Fig. 1f) (to the SSW of the volcano, population: 52 000 inhabitants), Guroymak town (to the SW of the volcano, population: 14 868) and Ahlat city (to the NE of the volcano, population: 22 000). Around Nemrut Volcano, about 135 000 inhabitants could be affected by future eruptions of this poorly known and unsurveyed volcano. For that reason, we undertook image analysis, combined with field work observations, of the possible impact areas and described transport pathways of volcanic materials of future eruptions.

### 3.1. Methodology

We used three-band SPOT images, taken by the SPOT-2 satellite with the HRV instrument on 8/9/1997 (Fig. 1). Then, we constituted the image in RGB format using the third, second and first bands, respectively. The image was georeferenced using 49 ground control points and then the method of LUT (Look Up Table detailed in Richards, 1993) was applied using linear stretching.

In addition to the satellite image, a DEM (Digital Elevation Model), which covers $22 \times 28$ km of surface area and has a resolution of 40 m, was produced by digitizing 1/25 000 scaled topographic maps of the relevant area. Then, the digitized map was linearly interpolated to have a defect-free surface of the volcano. Finally, a raster image of the DEM was generated for geomorphological analysis.

Hierarchical cluster analysis was applied as geostatistical method to Nemrut Volcano. This procedure attempts to identify relatively homogeneous groups of cases (or variables) based on selected characteristics, using an algorithm that starts with each case (or variable) in a separate cluster and combines clusters until only one is left. This procedure was applied in two steps. In the first step, each valley was grouped with respect to its topographic elevations and slope values in each processed point. Then, the average slope values of groups and the slope values of the transition points between the groups (break points) were computed. As a second step, cluster analysis was applied to the groups of the first step to have homogeneous areal groups of slope values. Then, the valley groups were interpolated using kriging methods and the flanks of Nemrut Volcano were divided into four zones (green, yellow, pink and red).

### 3.2. Application and interpretation

First we realized a slope visualization (Fig. 3a) (the method used is detailed in Wood, 1996). The western flank of Nemrut is steeper than the others, and this flank hosts predominantly lava facies. The other flanks, especially the southern and eastern ones, mostly occupied by pyroclastics, represent irregular surfaces due to erosional factors. The drainage pattern of the volcano (Fig. 3b) shows that the valleys are radially distributed from the center. The deepest and longest ravines are situated on the western and southern flanks, and continue to Tatvan city.

To classify the steep valleys, the slope image

Fig. 4. Visualization of risk factors and the impact areas of future eruptions. (a) Illustration of deepest and longest valleys as the most dangerous pathways. Contour map based on calculated $H/L$ values. (b) Estimation for each slope value of valleys and valley classification according to their importance. (c) Overlapped spot image and DEM of Mount Nemrut, creating 3D near-real visualization. The risk zones and possible impact areas, during a volcanic event related to Mount Nemrut, deduced by morphological analysis (slope values and $H/L$ parameters): green zone, high slope values which will be mantled by the products if an eruption occurs; yellow zone, transitional zone from topography mantling to channeling; pink zone, smaller slope values where the fan-style behavior of transported material will be expected; red zone, the possible deposition field of transported mass. Note that the settlements are located within the pink and red zones.

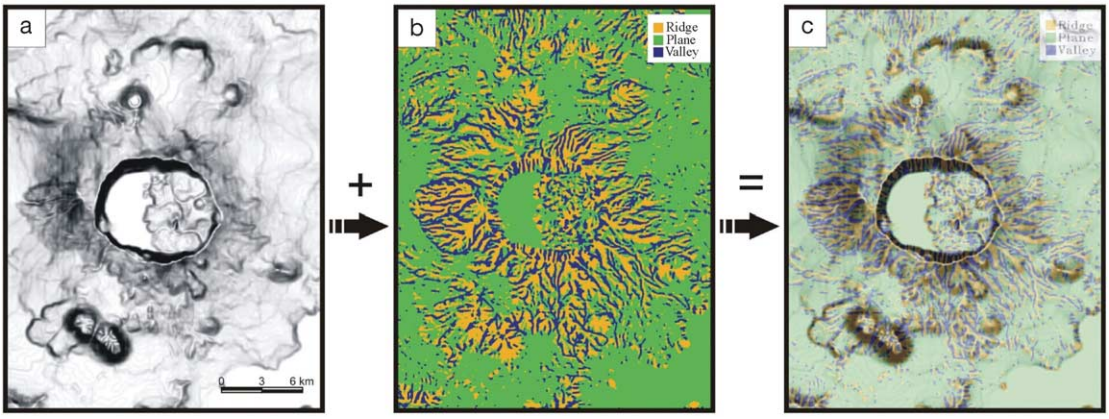
a
b
Ridge
Plane
Valley
c
0 3 6 km

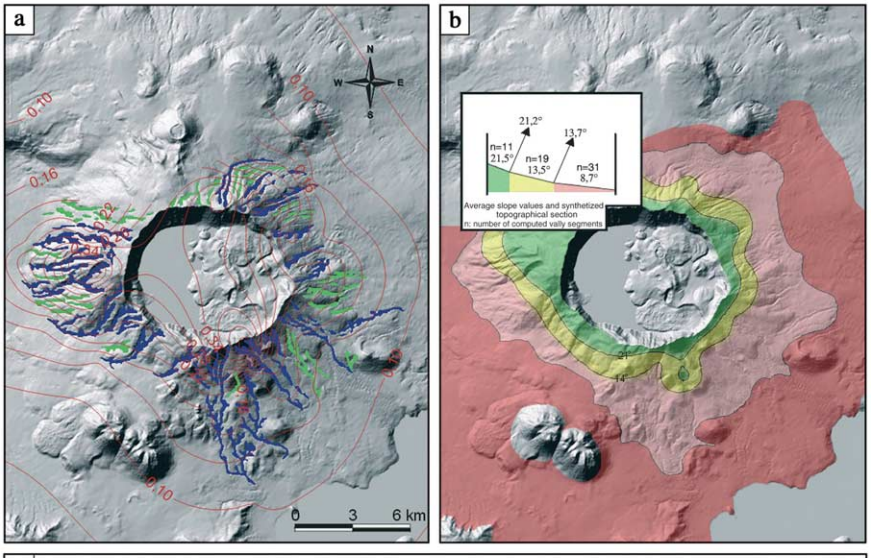
a
N
W
E
S
0.10
0.16
0 3 6 km
b
21.2°
13.7°
n=11
21.5°
n=19
13.5°
n=31
8.7°
Average slope values and synthetized topographical section
n: number of computed vally segments

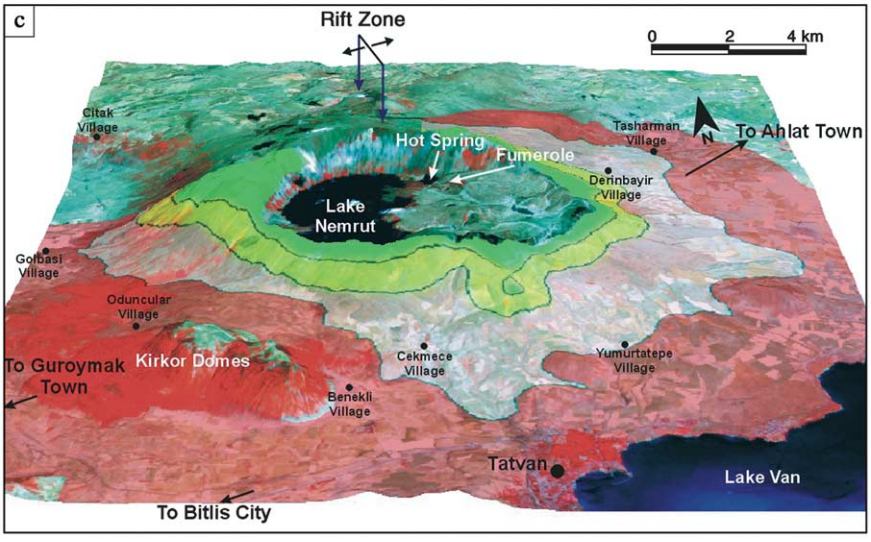
c
Rift Zone
0 2 4 km
Citak Village
Hot Spring
Fumerole
Tasharman Village
To Ahlat Town
Derinbayir Village
Lake Nemrut
Golbasi Village
Oduncular Village
To Guroymak Town
Kirkor Domes
Cekmece Village
Yumurtatepe Village
Benekli Village
Tatvan
Lake Van
To Bitlis City

Table 1
Physical characteristics of selected valleys and the results of geostatistical classification

| Valley | Processed data points | Length of valley (m) | Max. depth (m) | First cluster analysis | Mean slope values of first cluster analysis groups | Breaking point slope value between first and second groups | Breaking point slope value between second and third groups | Second cluster analysis |
|---|---|---|---|---|---|---|---|---|
| *Western and southwestern flanks* | | | | | | | | |
| v1 | 140 | 5895 | 36 | 1 | 17.4 | 16.2 | | y |
| | | | | 2 | 9.8 | | | p |
| v2 | 160 | 4958 | 144 | 1 | 16.9 | 26.26 | 15.55 | y |
| | | | | 2 | 17.8 | | | y |
| | | | | 3 | 6.2 | | | p |
| v3 | 151 | 4301 | 133 | 1 | 24.1 | 22.14 | 23.4 | g |
| | | | | 2 | 15.7 | | | y |
| | | | | 3 | 8.3 | | | p |
| v4 | 190 | 5235 | 204 | 1 | 24.9 | 25.57 | 12.03 | g |
| | | | | 2 | 19.6 | | | y |
| | | | | 3 | 7.4 | | | p |
| v5 | 219 | 6009 | 65 | 1 | 14.5 | 18.88 | 14.57 | y |
| | | | | 2 | 14.7 | | | y |
| | | | | 3 | 7.8 | | | p |
| v6 | 132 | 3834 | 94 | 1 | 11.9 | 18.95 | 7.11 | y |
| | | | | 2 | 6.5 | | | p |
| | | | | 3 | 4.7 | | | p |
| v7 | 111 | 3054 | 100 | 1 | 13.1 | 10.6 | 15.99 | y |
| | | | | 2 | 8.1 | | | p |
| | | | | 3 | 7.2 | | | p |
| *Southern and southeastern flanks* | | | | | | | | |
| v8 | 313 | 9114 | 127 | 1 | 17.3 | 12.62 | 7.39 | y |
| | | | | 2 | 8.9 | | | p |
| | | | | 3 | 3.3 | | | p |
| v9 | 209 | 7119 | 121 | 1 | 23.9 | 23.59 | 8.64 | g |
| | | | | 2 | 10.4 | | | p |
| | | | | 3 | 4.5 | | | p |
| v10 | 287 | 7680 | 135 | 1 | 25.7 | 23.92 | 9.68 | g |
| | | | | 2 | 9.4 | | | p |
| | | | | 3 | 4.0 | | | p |
| v11 | 180 | 4513 | 135 | 1 | 13.1 | 10.68 | 7.91 | y |
| | | | | 2 | 8.1 | | | p |
| | | | | 3 | 5.5 | | | p |
| v12 | 155 | 4306 | 142 | 1 | 14.1 | 16.75 | 8.26 | y |
| | | | | 2 | 7.8 | | | p |
| | | | | 3 | 4.9 | | | p |
| v13 | 123 | 3445 | 20 | 1 | 9.6 | 11.11 | 11.68 | p |
| | | | | 2 | 8.2 | | | p |
| | | | | 3 | 4.9 | | | p |
| v14 | 192 | 5278 | 80 | 1 | 10.2 | 7.31 | 10.72 | p |
| | | | | 2 | 6.3 | | | p |
| | | | | 3 | 5.1 | | | p |
| v15 | 251 | 7153 | 17 | 1 | 11.4 | 12.46 | 6.08 | y |
| | | | | 2 | 6.5 | | | p |
| | | | | 3 | 3.9 | | | p |
| *Northern and northeastern flanks* | | | | | | | | |
| v16 | 97 | 2591 | 23 | 1 | 13.5 | 18.97 | 11.34 | y |
| | | | | 2 | 12.7 | | | y |
| | | | | 3 | 7.2 | | | p |
| v17 | 107 | 2692 | 36 | 1 | 11.3 | 16.03 | 9.87 | y |

Table 1 (*Continued*).

| Valley | Processed data points | Length of valley (m) | Max. depth (m) | First cluster analysis | Mean slope values of first cluster analysis groups | Breaking point slope value between first and second groups | Breaking point slope value between second and third groups | Second cluster analysis |
|---|---|---|---|---|---|---|---|---|
| | | | | 2 | 10.0 | | | p |
| | | | | 3 | 4.9 | | | p |
| v18 | 94 | 2722 | 47 | 1 | 12.1 | 24.08 | | y |
| | | | | 2 | 7.3 | | | p |
| v19 | 99 | 2646 | 35 | 1 | 27.7 | 18.18 | | g |
| | | | | 2 | 10.4 | | | p |
| v20 | 94 | 3229 | 40 | 1 | 22.0 | 12.98 | | g |
| | | | | 2 | 7.1 | | | p |
| v21 | 132 | 3576 | 40 | 1 | 18.6 | 21.31 | | y |
| | | | | 2 | 7.2 | | | p |
| v22 | 136 | 3556 | 44 | 1 | 24.4 | 20.91 | 7.5 | g |
| | | | | 2 | 13.5 | | | y |
| | | | | 3 | 6.0 | | | p |

Abbreviations: g, green; y, yellow; p, pink.

and valley visualization were overlapped (Fig. 3c). In the case of an eruptive event or a debris flow, transported materials will probably travel down these valleys. The risk factors were estimated for each slope value of the valleys and were classified as first degree and second degree according to their importance (Fig. 4a). Twenty-two valleys were selected between the deepest and longest ones as the most dangerous pathways. Although they are numerous, the channels are unified in three main directions: to Tatvan, Bitlis–Guroymak and Ahlat cities. The slope values were classified in four groups (Fig. 4b) using the statistical method of Hierarchical Cluster Analysis (realized by 3572 slope and altitude values) based on 'between-groups linkage and squared Euclidean distance' parameters. The results, except the lowlands, are summarized in Table 1. To complete the morphological analysis, we computed for 22 selected valleys and for each settlement the Heim parameters $H/L$ (vertical drop/runout distance between the source and the deposition area of possible debris flows). For those calculations, the end of each valley and also each settlement were considered as depositional areas for expected flood flow. Although the values obtained do not correspond to the mobility of any product, we evaluated the mobility character of possible floods under topographical influences. In their works on hazard estimation of the possible pyroclastic flow disasters, Itoh et al. (2000) also suggest that topography and starting direction of flood strongly influence the impact area more than the volume of pyroclastics and discharge rate. The contour map of those calculations presented in Fig. 4a confirms the role of topographical influences on possible impact areas. The contours are condensed in three directions (WSW, SSE, NNE) and show clearly that if any volcanic debris occurs, these products will probably travel in those directions. The sectoral average values obtained from each valley are 0.202 for the WSW flank, 0.115 for the SSE flank and 0.185 for the NNE flank. The details are given in Table 2. Thouret et al. (2000) plot $H$ vs. $L$ on a diagram for the small-volume pyroclastic flows, large-volume pyroclastic flows, debris flows and cold rock avalanches of Merapi and Unzen volcanoes. They clearly show that most of the large-volume pyroclastic flows and debris flows generated by Merapi and Unzen have $H/L$ ratios between 0.1–0.02, while $H/L$ values of small-volume pyroclastic flows and cold rock avalanches range between 0.5 and 0.1. On the other hand, Capra et al. (2002) also calculate $H/L$ ratios of debris flows and debris avalanches for Mexican volcanoes and point out that $H/L$ ratios are 0.03–0.05 for debris flows and $H/L$ values of less mobile debris avalanches are between 0.13 and 0.09. Comparing those values with Mount Nemrut data, the flanks of Nemrut and

Table 2
Calculated Heim parameters $H/L$ for the valleys and settlements around the volcano

| Valley | $H/L$ ratio for the flanks | | | Settlement | $H/L$ |
|---|---|---|---|---|---|
| | Green–yellow transition | Yellow–pink transition | Pink–red transition | | |
| *Western and southwestern flanks* | | | | | |
| v1 | 0.200 | 0.242 | 0.214 | Golbasi | 0.155 |
| v2 | 0.240 | 0.264 | 0.228 | Oduncular | 0.104 |
| v3 | 0.380 | 0.421 | 0.276 | Citak | 0.086 |
| v4 | 0.466 | 0.397 | 0.230 | Guroymak | 0.058 |
| v5 | 0.238 | 0.241 | 0.179 | | |
| v6 | 0.201 | 0.207 | 0.133 | | |
| v7 | 0.251 | 0.183 | 0.154 | | |
| *Southern and southeastern flanks* | | | | | |
| v8 | 0.282 | 0.187 | 0.114 | Yumurtatepe | 0.158 |
| v9 | 0.129 | 0.151 | 0.101 | Cekmece | 0.150 |
| v10 | 0.472 | 0.179 | 0.109 | Benekli | 0.130 |
| v11 | 0.229 | 0.178 | 0.145 | Tatvan | 0.101 |
| v12 | 0.240 | 0.156 | 0.124 | Bitlis | 0.049 |
| v13 | 0.168 | 0.159 | 0.122 | | |
| v14 | 0.178 | 0.134 | 0.110 | | |
| v15 | 0.203 | 0.138 | 0.102 | | |
| *Northern and northeastern flanks* | | | | | |
| v16 | 0.249 | 0.234 | 0.193 | Derinbayir | 0.125 |
| v17 | 0.196 | 0.185 | 0.151 | Tasharman | 0.079 |
| v18 | 0.169 | 0.208 | 0.166 | Ahlat | 0.033 |
| v19 | 0.307 | 0.298 | 0.213 | | |
| v20 | 0.191 | 0.269 | 0.191 | | |
| v21 | 0.301 | 0.317 | 0.204 | | |
| v22 | 0.402 | 0.267 | 0.181 | | |

most of the settlements around the volcano have $H/L$ values $>0.1$. It means that considering the literature data on Merapi, Unzen and Mexican volcanoes, the flanks of Mount Nemrut will be affected by the future volcanic event. Some settlements like Ahlat, Tasharman, Bitlis, Guroymak, Citak have $H/L$ values less than 0.1. According to an assumption based on literature data, we can suggest that those settlements will be threatened only by large-volume, highly mobile pyroclastic flows and/or air-falls if they occur. On the other hand, Ahlat town will probably be less threatened from an event, because it is located in the flatland. It is difficult to consider that the surge or flow products could reach Ahlat city if a future eruption will occur as a hydrovolcanic one or cold debris generated by strong rainfalls.

Transported volcanic materials (erupted or cold debris) could reach the city center of either Tatvan or Bitlis and Guroymak or both. We emphasize that the altitude of the SW part of the Kirkor domes, in the direction of Bitlis valley, is topographically 100 m below Lake Van (1646 m).

Finally, the spot image and DEM of Nemrut were overlapped, creating 3D near-real visualization (Fig. 4c). On this image, cluster classification is shown with different colors as potential risk zones as a function of their average slope and $H/L$ values which may affect the mobility of transported material. The expected behavior of transported material which would be produced during the next volcanic event on different zones of Mount Nemrut is summarized as follows.

A green color corresponds to high slope values and this area could be mantled by eruptive deposits. There are no settlements in the green zone, so the expected impact of the next event will only affect the environment rather than the human life in this zone. The average $H/L$ ratio of this zone is 0.26. The yellow zone is a transitional zone from topography mantling to channeling. Its average $H/L$ ratio is close to 0.22. The average

slope values and $H/L$ ratios of the green and yellow zones lead us to suppose that those zones will be affected even from small-scale rock falls and less mobile, highly viscous transported material. The pink zone, where slope values are relatively smaller than in the previous zones ($<14°$), will witness the fan-style behavior of transported material which could probably destroy mainly Tatvan and/or Bitlis city. The red zone is the possible deposition field of transported mass. The settlements like the villages, town and cities are mainly situated in the pink and the red zones (Fig. 4c) where the slope values are gentle and most of those settlements are located at the end of the valleys. Cole et al. (1999) pointed out that the settlements within valleys or at valley mouths are particularly vulnerable to damage from tephra remobilization both during and after an explosive eruption of Furnas Volcano, Azores. In addition, Hall et al. (1999) emphasized how the valleys drain pyroclastic flows and debris flows on Tungurahua Volcano (Ecuador) and their role in the risk over Banos. In the light of our morphological analysis, we conclude that the volcano flanks are open to risks generated from all kinds of volcanic events, while some settlements which have $H/L$ values less than 0.1 will be threatened if a debris flow is triggered.

## 4. Discussion and conclusion

Mount Nemrut stratovolcano is located in an active tectonic context and releases mantle-derived gases. However, the last eruption of Mount Nemrut is known to have occurred in 1441 (Oswalt, 1912; Pfaffengolz, 1950; Ozpeker, 1973; Féraud, 1994; Yilmaz et al., 1998), but the live description of the last eruption of Nemrut in a book written in 1597 proves that the volcano was very active about 400 years ago. Additionally, the recent publication of Karakhanian et al. (2002), based on the Armenian Chronicles, shows that Mount Nemrut has had some historical volcanic activities. On the other hand, a study on Lake Van varve records for the past 10 420 years (Kempe and Degens, 1978) described the volcanic products of the 1441 AD eruption based on the sediment core sections as light-colored volcanic tuff rather than the dark-colored products emitted from the rift zone in 1441. So, in 1441, Mount Nemrut probably produced the light-colored tuffs which are actually present on the southern flank and within the caldera, and were related to a phreatomagmatic eruption.

According to the volcanological past of Mount Nemrut, two major hypotheses may be proposed for the expected eruption: intracaldera volcanism or flank eruption.

If the eruption occurs within the caldera, it will be phreatomagmatic and destructive because of the presence of water (about 1 $km^3$) within the caldera. The hot water mixed with pyroclastics will form mud flows, as occurred in the eruption of Nevado del Ruiz (Colombia) where about 25 000 people were killed in 1985. On the other hand, the region is high enough to have lots of snow during winter. This is also very dangerous, because if the magmatic gases heat snow by several degrees, debris flows can be generated.

The other possibility is a flank eruption. If an eruption occurs during winter, the same danger mentioned above could be produced. If not, the lava effusions could destroy the lands, as far as the city of Tatvan. Or, the rift zone could be reactivated, producing some lava flows.

As summarized above, the major risk for Mount Nemrut is its capability to produce small or large-volume pyroclastic flows and/or debris flows. This poorly known active volcano has been morphologically analyzed and the results are speculative. Twenty-two important valleys were distinguished. The maximum depth of some valleys reaches 200 m. The valleys are localized in three zones: the WSW flank where the deeper valleys are present, the SSE flank where the longest valleys are located, and the NNE flank where the valley depths and lengths are less important. Based on the morphological analysis we propose that Mount Nemrut Volcano has four danger zones, illustrated in Fig. 4c. The green and yellow zones will be affected by all types of event such as small or large-volume pyroclastic flows, cold or hot debris flows, surges or cold rock avalanches. The settlements are situated in the pink and red zones, which will probably be

threatened by channeled products. Considering the water presence within the caldera, debris flows may be generated during the next volcanic activity. Debris flows normally fill depressions and may attain their maximum thickness some distance from the edifice, where valleys widen and gradients become lower, as observed at Nevado de Toluca Volcano by Capra and Macias (2000). In this case those debris flows will use the valleys, be deposited in lowlands and probably destroy settlements.

Finally, Mount Nemrut represents a real danger for 135 000 people that live in the area and it is necessary to survey this volcano. So, a seismic survey combined with periodical water and gas sampling and analyzing will be proposed. An alert code system and civil evacuation plans need to be established.

## Acknowledgements

This work benefited from a research grant of Hacettepe University Research Foundation (Project No. 01 01 602 020). It was also financially supported by UMR-CNRS 6524. Prof. L. Wilson (Editor), Dr. Marta Calvache and an anonymous reviewer provided useful comments and ideas to the manuscript.

## References

Capra, L., Macias, J.L., 2000. Pleistocene cohesive debris flows at Nevado de Toluca volcano, Central Mexico. J. Volcanol. Geotherm. Res. 102, 149–168.

Capra, L., Macias, J.L., Scott, K.M., Abrams, M., Garduno-Monroy, V.H., 2002. Debris avalanches and debris flows transformed from collapses in the Trans-Mexican Volcanic Belt, Mexico – behavior, and implications for hazard assessment. J. Volcanol. Geotherm. Res. 113, 81–110.

Cole, P.D., Guest, J.E., Queiroz, G., Wallestein, N., Pacheco, J.M., Gaspar, J.L., Ferreira, T., Duncan, A.M., 1999. Styles of volcanism and volcanic hazards on Furnas volcano, Sao Miguel, Azores. J. Volcanol. Geotherm. Res. 92, 39–53.

Dewey, J.F., Hempton, M.R., Kidd, W.S.F., Saroglu, F., Sengor, A.M.C., 1986. Shortening of continental lithosphere: the neotectonics of Eastern Anatolia – a young collision zone. In: Coward, M.P., Ries, A.C. (Eds.), Collision Tectonics. Geol. Soc. Spec. Publ. 19, pp. 3–36.

Ercan, T., Fujitani, T., Matsuda, J.I., Notsu, K., Tokel, S., Ui, T., 1990. Dogu ve Guneydogu Anadolu Neojen–Kuvaterner volkaniklerine iliskin yeni jeokimyasal, radyometrik ve izotopik verilerin yorumu. MTA Dergisi 110, 143–164.

Féraud, J., 1994. Les volcans actifs de Turquie. Guide Géologique et itinéraires d'excursions. Mémoire de l'Association Volcanologique Européenne (LAVE), pp. 85–101.

Hall, M.L., Robin, C., Beate, B., Mothes, P., Monzier, M., 1999. Tungurahua Volcano, Ecuador: structure, eruptive history and hazards. J. Volcanol. Geotherm. Res. 91, 1–21.

Itoh, H., Takahama, J., Takahashi, M., Miyamoto, K., 2000. Hazard estimation of the possible pyroclastic flow disasters using numerical simulation related to the 1994 activity at Merapi Volcano. J. Volcanol. Geotherm. Res. 100, 503–516.

Karakhanian, A., Djrbashian, R., Trifonov, V., Philip, H., Arakelian, S., Avagian, A., 2002. Holocene-historical volcanism and active faults as natural risk factors for Armenia and adjacent countries. J. Volcanol. Geotherm. Res. 113, 319–344.

Kempe, S., Degens, E.T., 1978. Lake Van varve record: The past 10,420 years. In: Degens, Kurtman (Eds.), The Geology of Lake Van. MTA yayinlari 169, pp. 56–63.

Nagao, K., Matsuda, J.I., Kita, I., Ercan, T., 1989. Noble gas and carbon isotopic composition in Quaternary volcanic area in Turkey. Jeomorfoloji Dergisi 17, 101–110.

Oswalt, F., 1912. Armenian. Handbuch der regionalen Geologie, vol. 10. Heidelberg.

Ozpeker, I., 1973. Nemrut yanardaginin petrojenezi. ITU Mad. Fak. 3–14, 70 pp.

Pearce, J.A., Bender, J.F., De Long, S.E., Kidd, W.S.F., Low, P.J., Guner, Y., Saroglu, F., Yilmaz, Y., Moorbath, S., Mitchell, J.J., 1990. Genesis of collision volcanism in eastern Anatolia, Turkey. J. Volcanol. Geotherm. Res. 44, 189–229.

Pfaffengolz, K.N., 1950. Über die Entstehung der Seen: Sewan (Armenien), Wan (Anatolien) und Urmia (Iran). Mitteilungen der Akademie der Wissenschaften USSR, Geol. Serie, pp. 125–138.

Richards, J.A., 1993. Remote Sensing Digital Image Analyis: An Introduction. Springer, Berlin, 340 pp.

Serefhan, 1597. Serefname: Kurt tarihi (translated from arabic to turkish by M. Emin Bozarslan), 4th edn. (1990). Hasat yayinlari, 544 pp.

Thouret, J.C., Lavigne, F., Kelfoun, K., Bronto, S., 2000. Toward a revised hazard assessment at Merapi volcano, Central Java. J. Volcanol. Geotherm. Res. 100, 479–502.

Wood, J., 1996. The geomorphological characterization of digital elevation models. Ph.D. Thesis, Univ. of Leicester.

Yilmaz, Y., Saroglu, F., Guner, F., 1987. Initiation of the neomagmatism in East Anatolia. Tectonophysics 134, 177–199.

Yilmaz, Y., Guner, Y., Saroglu, F., 1998. Geology of the Quaternary volcanic centers of the east Anatolia. J. Volcanol. Geotherm. Res. 85, 173–210.